

Hybrid Steam Generation for Industry Using Linear Fresnel Solar Collectors and High Temperature Heat Pump

Antonio Famiglietti¹, Ruben Abbas¹

¹Thermal Energy for Sustainability (TE4S) Group, Escuela Técnica Superior de Ingenieros Industriales, Departamento de Ingeniería Energética, Universidad Politécnica de Madrid, Madrid (Spain)

Abstract

Although the ongoing energy transition is dominated by renewable electricity production, most of industrial energy consumption remains in form of heat, mostly provided by fossil fuel combustion. Relevant industrial sectors as food and beverage, textile, chemical, pulp and paper, among others, present large heat consumption in the low and medium temperature range. Steam is used as heat transfer fluid in a large variety of processes.

Concentrating solar thermal technologies are suitable renewable heat sources able to replace fossil fuel and are recently receiving increasing attention and market share. Besides, electricity-driven Heat Pump are able to provide heat using either renewable or grid electricity whenever waste or unused low-grade heat is available. Although commercial industrial Heat Pumps are limited to low temperature applications, recent developments are bringing High Temperature Heat Pumps to market, able to provide heat above 150 °C up to 280 °C. In this study Linear Fresnel Solar Collectors and High Temperature Heat Pumps are considered as heat sources for steam generation for industrial process. Energetic and economic analysis is performed for different locations under various design constraints.

Keywords: Solar Heat for Industrial Processes, Steam Generation, High temperature Heat Pump, Thermal Energy Storage

1. Introduction

Decarbonization of the industrial sector is crucial to achieving sustainability goals and reducing industrialized economies' dependence on fossil fuels. According to IRENA (International Renewable Energy Agency), 74% of industrial energy demand is heat (85 EJ), mainly provided by consuming fossil fuels. Around 50% of industrial heat is required at low temperature (< 150 °C) and medium temperature (150-400 °C), consumed in a wide variety of industrial processes. ST Solar Thermal technologies can provide heat in different temperature ranges, with good performance and reasonable costs.

Linear concentrating solar technologies such as parabolic troughs and linear Fresnel collectors can operate in the medium temperature range with high efficiencies. They offer high performance and are available in different scales due to their modularity at decreasing costs. Despite their technological maturity and huge market potential, ST solar thermal technologies still play a marginal role as an industrial heat source. Among the barriers to the massive implementation of technology, economic competitiveness with conventional sources plays a fundamental role.

Solar photovoltaic (PV) energy is gaining market share at increasingly lower costs, being the dominant solar technology in the electricity sector. The application of photovoltaic energy in industry is intended to cover not only conventional electrical demand, but its applications to process heat are becoming more and more interesting. Furthermore, the electrification of industrial thermal demand is strategic in a context with high penetration of renewables in the electrical grid. "Power-to-heat" solutions, capable of efficiently using solar and renewable electricity for industrial heat supply today are extremely necessary and attractive. Although commercial industrial heat pumps are limited to low temperature applications, recent developments are bringing to the market High Temperature Heat Pumps (HT-HP) capable of providing heat above 150 °C

(Arpagaus et al., 2018).

This study analyzes the generation of steam for industrial use using Fresnel-type concentration technology and the high-temperature heat pump powered by photovoltaic solar energy. For this purpose, a reference industrial user is considered, characterized by the specifications of the steam network (saturated steam pressure, condensate return temperature, among others).

The integration scheme chosen for the study is the “indirect” generation of steam, in parallel to a conventional natural gas steam boiler. The indirect generation of solar steam implies the need for a BOP (Balance of Plant) system consisting of a “kettle reboiler Steam Generator (SG)” and auxiliary equipment. The kettle steam generator is fed by condensate from the industrial network while the heat is supplied through a primary heat transfer fluid. The saturated steam generated by the kettle is injected into the industrial distribution network. In this study, the Heat Transfer Fluid (HTF) is pressurized water, being a commonly used option in the expected temperature range (150-200 °C). Different configurations of solar heating of the primary fluid are analyzed. Concentrating Solar Thermal (CST) and high temperature Heat Pump (HP) powered by a Photovoltaic (PV) are considered as heat sources, either alone or combined in hybrid scheme.

The first option in Fig.1 uses a Concentrating Solar Thermal (CST) solar field as heat source. In the second scheme, shown in Fig. 2, a high temperature Heat Pump (HP) powered by a Photovoltaic (PV) solar field is the heat source. A comparative energetic and economic analysis is carried out considering the CST and PV-HP schemes through annual simulation on a large number of locations in European countries.

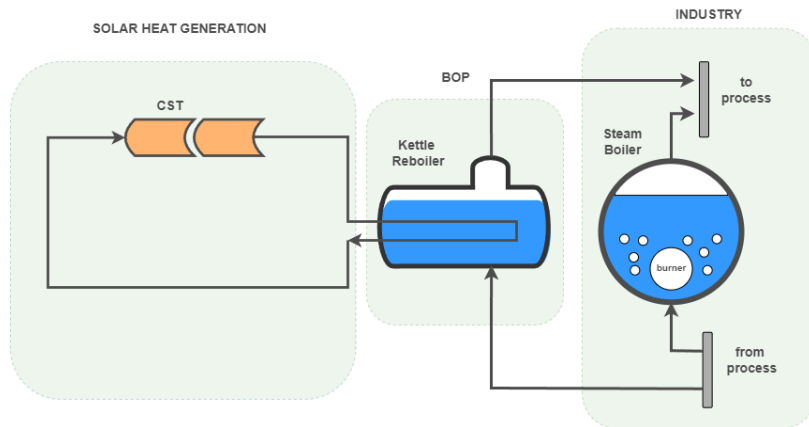


Fig.1: Indirect steam generation using CST as heat source.

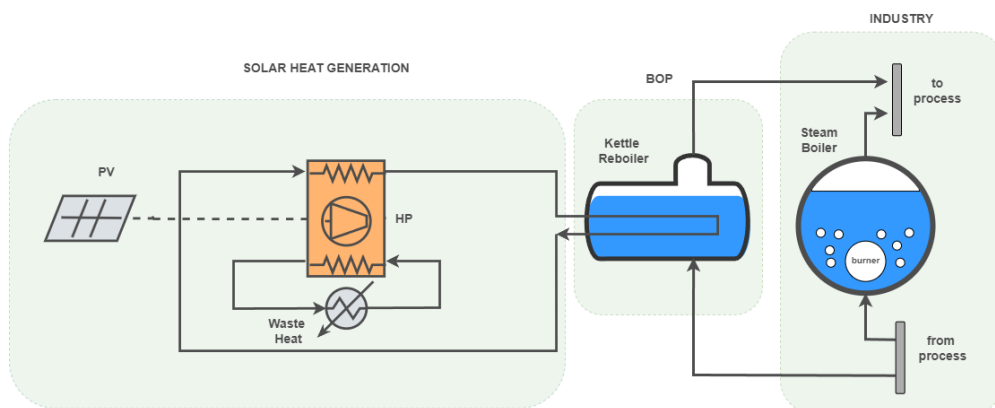


Fig.2: Indirect steam generation using PV-HP as heat source

Advanced hybrid scheme including either the CST and PV-HP as heat source and a sensible Thermal Energy Storage TES is analyzed, Fig.3. For the various configurations, hourly simulations are carried out across the typical meteorological year of the localities of interest, to evaluate the main energy indicators (annual solar fraction) and economic indicators (Levelized Cost of Heat, LCOH). A parametric analysis allows to establish the impact of the main design and operational parameters on energy and economic indicators.

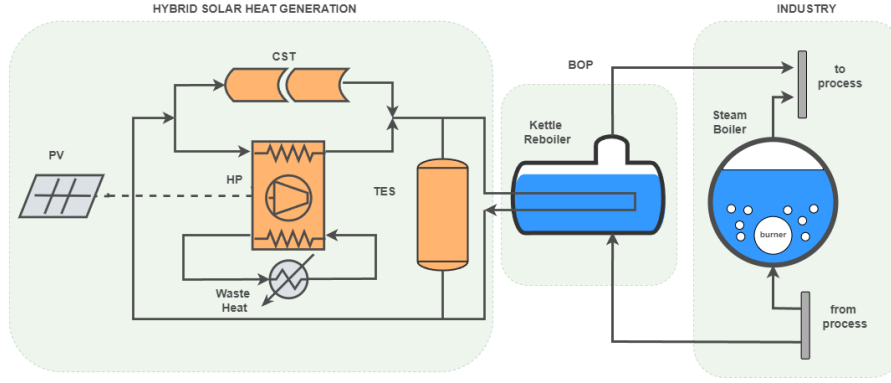


Fig.3: Hybrid scheme for indirect solar generation using CST and PV-HP as heat source including TES

2. Numerical model

The numerical models have been implemented in Python and include the SG vapor generation, the concentrating solar field CST, the photovoltaic solar field PV, the heat pump HP, the thermal storage TES, besides the control algorithm appropriate for each configuration. The economic model of the considered components is also implemented.

2.1. Steam generation SG

Solar steam generation is carried out in parallel with the main steam generator (Boiler, BO) via a kettle steam generator (SG). The steam pressure p_s and the temperature T_s are defined according to parameters of the boiler, as well as the water inlet temperature T_{cond} (condensate return). The steam flow rate \dot{m}_s and the corresponding thermal power \dot{Q}_s are obtained from the design values $\dot{m}_{s,d}$ and $\dot{Q}_{s,d}$ and the hourly profile of the industrial demand. Other design parameters of the SG are the inlet and outlet temperatures of the liquid side $T_{l,in}$, $T_{l,out}$. The primary liquid is pressurized water. The pressure on the liquid side p_l is set above the saturation temperature to avoid two-phase flow, $p_l = p_{sat}(T_{l,in} + \Delta T_{safe})$. Outlet water temperature $T_{l,out}$ is defined starting from steam temperature T_s as $T_{l,out} = T_s + \Delta T_{HX}$, and $T_{l,in} = T_{l,out} + \Delta T_l$.

The estimation of the installation costs C_{SG} of the SG steam generator is obtained starting from the area of the heat exchanger A_{SG} , considering a heat transfer reference value $U_{SG} = 1400 \text{ Wm}^{-2}\text{K}^{-1}$. Corrective factors that consider the pressure F_p and the material F_M are applied to the base cost C_B , (Seider et al.).

$$C_{SG} = C_B F_p F_M C_{Eur} C E_{index} \quad (\text{eq. 1})$$

$$C_B = \exp(12.3310 - 0.8709 \ln(A_{SG}) + 0.09005 (\ln(A_{SG}))^2) \quad (\text{eq. 2})$$

$$F_p = 0.9803 + 0.018 \left(\frac{p_{SG}}{100} \right) + 0.0017 \left(\frac{p_{SG}}{100} \right)^2 \quad (\text{eq. 3})$$

$$F_M = a + \left(\frac{A_{SG}}{100} \right)^b \quad (\text{eq. 4})$$

with $a=2.7$ and $b=0.07$ of stainless steel, and C_{Eur} conversion factor USD to Eur, A_{SG} in ft^2 and pressure p_{SG} in psig . The $C E_{index}$ accounts for inflation, according to CEPCI index (Maxwell).

2.2 Concentrating Solar Thermal CST

The CST field is defined based on the collector features, the configuration of the loops and their orientation. The collector is a commercial linear Fresnel collector LFC (Solatom), equipped with a single standard evacuated tube receiver, whose main technical data are reported in Tab.1.

Tab. 1. CST parameters and data

Length of the module	L_m	5.28 m
Aperture	W_a	5.00 m
Height	H_m	2.72 m
Active area of the module	A_m	26.40 m ²
Maximum optical efficiency	η_{op0}	0.632
Internal diameter receiver	D	0.066 m
External diameter receiver	D_{ex}	0.07 m

The solar field is defined by the number of LFCs assembled in series n_s in a straight row, while n_p rows are arranged in parallel. The LFC is modeled by calculating heat flux \dot{q}_s concentrated on the receiver perimeter $P_{ex} = D_{ex}\pi$, by means of an optical efficiency η_{op} including the Incidence Angle Modifiers IAMs.

$$\dot{q}_s = \frac{G_{bn}\eta_{op}A_c}{A_r} = \frac{G_{bn}\eta_{op}W_a}{P_{ex}} = G_{bn}\eta_{op}C \quad (\text{eq. 5})$$

$$\eta_{op} = \eta_{op0}IAM_T(\theta_T)IAM_L(\theta_L) \quad (\text{eq. 6})$$

The thermal power \dot{Q}_u generated by the fluid across a length L of the receptor is obtained according to (Duffie et al., 1985) using the collector efficiency factor F' and the heat dissipation factor F_R .

$$\dot{Q}_u = F_R L P_{ex} [\dot{q}_s - U_L(T_{in} - T_{amb})] = \dot{m}(h_{e_{ou}} - h_{e_{in}}) \quad (\text{eq. 7})$$

$$F' = \left[1 + \frac{U_L P_{ex}}{h_l P}\right]^{-1}; F_R = \frac{\dot{m} c_p}{L P_{ex} U_L} \left[1 - \exp\left(-\frac{L F' P_{ex} U_L}{\dot{m} c_p}\right)\right] \quad (\text{eq. 8})$$

The global heat transfer coefficient of the receiver tube $U_L(T_w, T_{amb})$ is obtained by means of a polynomial expression obtained from experimental data (Burkholder & Kutscher, 2009). Internal heat transfer h_l coefficient is computed from Gnielinski correlation. The length of the receiver is discretized into n_e elements for increasing the accuracy.

The solar field area is sized based on the required peak power \dot{Q}_{CST} which determine the solar multiple as $SM_{CST} = \dot{Q}_{CST}/\dot{Q}_{s,d}$. The number of loops n_p and their length L_d are adjusted to fit the required area.

The installation cost of solar field is obtained from an estimated cost per area $c_{CST} = 325 \text{ Eur m}^{-2}$. This cost is retrieved from the manufacturer's simulation tool (Ressspi, 2018) implemented by (Solatom), for a solar field of 50 modules without integration, applying the CEPCI inflation correction factor (Maxwell). Peak irradiance is $G_{bn,peak} = 1000 \text{ Wm}^{-2}$.

$$A_{CST} = \frac{\dot{Q}_{CST}}{G_{bn,peak}\eta_{op0}} = L_d W_a n_p \quad (\text{eq. 9})$$

$$C_{CST} = A_{CST} c_{CST} \quad (\text{eq. 10})$$

2.3 Solar photovoltaic field PV

The solar field is defined according to the electrical power required by the heat pump in nominal conditions P_d . The orientation is horizontal, being the most common option on industrial rooftops. The conversion efficiency of the solar cell is $\eta_{PV} = 0.20$, and a reference system efficiency of $\eta_{sys} = 0.86$, account for system losses such as losses in cables, power inverters, dirt on the modules, efficiency degradation with time. The

installation cost is obtained from the cost per kwp $c_{kwp} = 814 \text{ €/KWp}$, (IRENA, 2022).

$$A_{PV} = \frac{P_{PV,d}}{G_{bn,peak}\eta_{PV}\eta_{BOP}} \quad (\text{eq. 11})$$

$$C_{PV} = P_{PV,d}c_{kwp} \quad (\text{eq. 12})$$

2.4 High Temperature Heat Pump

The high-temperature heat pump considered is a pre-commercial Stirling-type model manufactured by Enerin (Enerin, n.d.). The real COP_{HP} of the hat pump is obtained from the ideal COP_{Carnot} , according to the efficiency η_{COP} reported by (Høeg et al., 2023), as function of the average temperatures of the heat source temperature $T_{source,m}$ and the heat sink temperature $T_{sink,m}$.

$$COP_{HP} = \frac{Q_h}{P_{HP}} = \frac{Q_h}{Q_h - Q_c} = COP_{Carnot}\eta_{COP} \quad (\text{eq. 13})$$

$$COP_{Carnot,h} = \frac{T_{sink,m}}{T_{sink,m} - T_{source,m}} \quad (\text{eq. 14})$$

The heat transfer fluid is pressurized water on both low and high temperature sides, with a maximum temperature glide of 25 °C and 40 °C respectively. The maximum temperature drop (lift) is indicated by the manufacturer is 200°C, with a maximum heat sink temperature of 250 °C. The heat supply capacity is between 0.3 MW and 10 MW, (Annex 58 Task 1). The installation cost is calculated from the unitary cost $c_{HP} = 700 \frac{\text{€}}{\text{kW}}$, as $C_{HP} = c_{HP}\dot{Q}_{HP}$. The HP is sized according to \dot{Q}_{HP} and solar multiple $SM_{HP} = \dot{Q}_{HP}/\dot{Q}_{s,d}$.

2.5 Thermal energy storage TES

The sensible thermal storage considered in this study is of the thermally stratified tank filled with pressurized water. The TES volume is sized based on the required storage hours h_{TES} and the design temperatures T_h and T_c , for the hot and cold side respectively. The V_{TES} volume is divided into several n_{tanks} with a maximum admissible tank height $H_{tank,max}$ and a shape factor F_{Sh} .

$$V_{TES} = \frac{3600 \dot{Q}_{s,d} h_{TES}}{\rho_l c p_l (T_h - T_c)} = V_{tank} n_{tank} \quad (\text{eq. 15})$$

$$D_{tank} = \left(\frac{n_{tank}^4}{\pi F_{Sh}} \right)^{\frac{1}{3}} ; H_{tank} = F_{Sh} D_{tank} \quad (\text{eq. 16})$$

Tank shell thickness e_{tank} is obtained from pressure and diameter, Eq (17), with $E = 0.85$, S and p_{tank} in psi, $S = 16000 \text{ psi}$ for stainless steel.

$$e_{tank} = \frac{p_{tank} D_{tank}}{2SE - 0.6p_{tank}} 0.0254 \quad (\text{eq. 17})$$

The cost of each tank is calculated considering the cost of the vessel C_{vessel} , of the liquid C_{liq} , thermal insulation C_{ins} , foundations C_{fou} , hydraulic and electrical equipment C_{AUX} , installation C_{inst} and overhead C_{oh} , elaborated starting from (Mostafavi Tehrani et al., 2017).

$$C_{PBTES} = C_{vessel} + C_{fluid} + C_{ins} + C_{fou} + C_{AUX} + C_{oh} + C_{inst}$$

Tab. 2: Economic parameters of TES

Vessel	C_{vessel}	4.5 €/kg
Insulation	C_{ins}	300 €/m ²
HTF	C_{fluid}	Agua 0.8 €/ m ³
Foundations	C_{fou}	1120 €/m ²
Electric and instrumentation, valves and fittings	C_{AUX}	390 €/m ³
Overhead	C_{oh}	10% of total
Installation	C_{inst}	20% of total

2.6 Levelized Cost of Heat LCOH

The Levelized Cost of Heat (LCOH) is used as the main economic indicator in this study. The LCOH is the heat generation cost, also the minimum price that must be sold to recover the installation costs (CAPEX) and the operation and maintenance costs (OPEX) during its useful life of the plant. It is defined in a similar way to the Level of Energy Cost LCOE used for the financial analysis of electricity production.

According to Task 54 of the IEA, the LCOH can be estimated in the following way, considering constant annual discount, Eq (18). If we assume $r_{dis} = 0.05$, $n_y = 25$ years, OPEX = 0.02 CAPEX .

$$CAPEX = C_{CST} + C_{TES} + C_{PV} + C_{HP} + C_{SG} \quad (\text{eq. 18})$$

$$LCOH = \frac{I_0 + \sum_{n_y=1}^{N_y} \frac{OPEX_{n_y}}{(1 + r_{dis})^{n_y}}}{\sum_{n_y=1}^{N_y} \frac{E_{n_y}}{(1 + r_{dis})^{n_y}}} \quad (\text{eq. 19})$$

3. Methodology

The models allow to carry out annual simulations considering the typical meteorological year for each location considered. Hence the simulation considers time interval of 1 hr, according to meteorological data. The load time profile of industry is considered constant in this study (24/7). The design parameter used for the simulation are defined as in Tab. 3, assuming 8 bar steam pressure (170 °C), a condensate return line temperature of 150 °C, a steam flow rate $\dot{m}_s = 1$ kg/s. The inlet/outlet temperature of tube side of the kettle SG liquid is set to 210/180 °C working with pressurized water at 23.4 bar. Considering the PV-HP, the heat pump needs a low temperature source, which is assumed here to be waste heat at 70 °C available at the factory. Under the current assumptions, the HP operates with a COP = 2.07.

Tab. 3: Design parameters for steam generation

Steam Pressure	8 bar
Steam Temperature	170 °C
Condensate Temperature	150 °C
Load Profile	24/7
Steam flow rate	1 kg/s
Load Thermal Power	2.14 MWh
ΔT_l	30°C
ΔT_{HX}	10°C
ΔT_{safe}	10°C
Orientation CST	N-S
Tilt PV	horizontal
Waste heat temperature HP	70 °C

Three main values obtained from the annual simulation are considered as KPIs in this study, being the annual solar fraction SF, the annual energy yield per unit of gross area occupied by solar field (either CST or PV) E_{area} , and the levelized cost of heat LCOH.

The analysis is first devoted to assessing the energetic and economic performance of CST and PV-HP steam generation scheme across European locations.

Then hybrid schemes are considered where both CST and PV-HP technologies are integrated to produce industrial steam according to layout in Fig.3. As design parameter, hybridization ratio R_{hy} is defined in this study to account for the proportions of installed power of CST and PV-HP respectively, Eq. (20). Hybrid solar multiple is defined for the hybrid scheme analogously to PV-HP and CST simple schemes, Eq.(21).

$$R_{hy} = \frac{\dot{Q}_{HP}}{\dot{Q}_{CST} + \dot{Q}_{HP}} \quad (\text{eq. 20})$$

$$SM_{hy} = \frac{\dot{Q}_{CST} + \dot{Q}_{HP}}{\dot{Q}_{s,d}} \quad (\text{eq. 21})$$

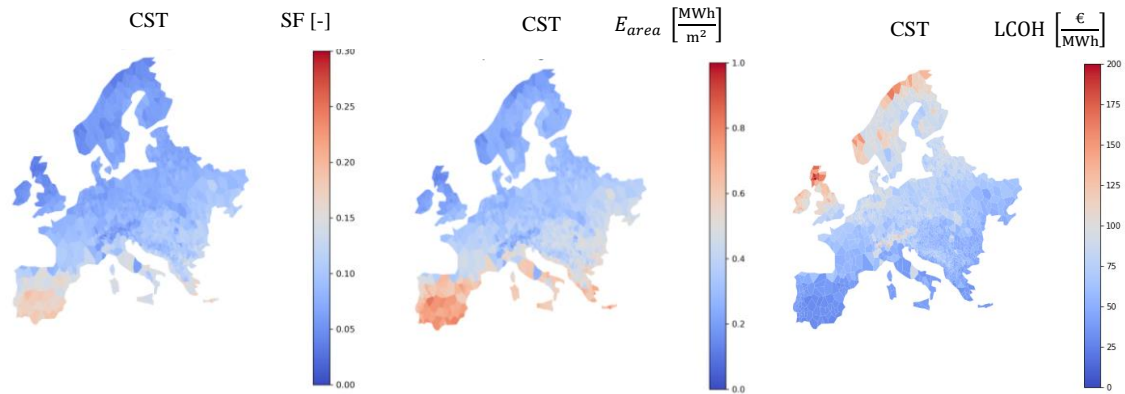
For $SM_{hy} = 1$ the thermal energy storage is not included in the layout. For higher SM_{hy} a proper TES volume is added in parallel to the PV-HP and CST heat generation.

In this study a criterion for TES sizing is implemented. First an attempt of sizing the volume V_{TES} is made on daily basis, defining the minimum volume $V_{TES,max}$ which allow to store the maximum daily energy excess. Then an economic criterion is applied to find and optimization factor F_{TES} which gives the minimum LCOH including the a $V_{TES} = V_{TES,max}F_{TES}$ in the scheme. In this study F_{TES} can assume discrete values from 0 to 2 with step of 0.20, in order to keep low computational cost.

4. Results

4.1 Comparative CST and PV-HP steam generation.

Annual simulations are carried out for the CST scheme as well for the PV-HP. The solar multiple is set to $SM = 1$ for both cases, so that no excess of energy is provided by the solar installation. The simulation is carried out for 50 random selected locations per each European country, for a total of 1350 locations. The results for the three selected KPIs are shown in Fig.4 as geographical heat maps. Moreover, the results are reported ordered by annual global horizontal irradiation (GHI) in Fig.4.



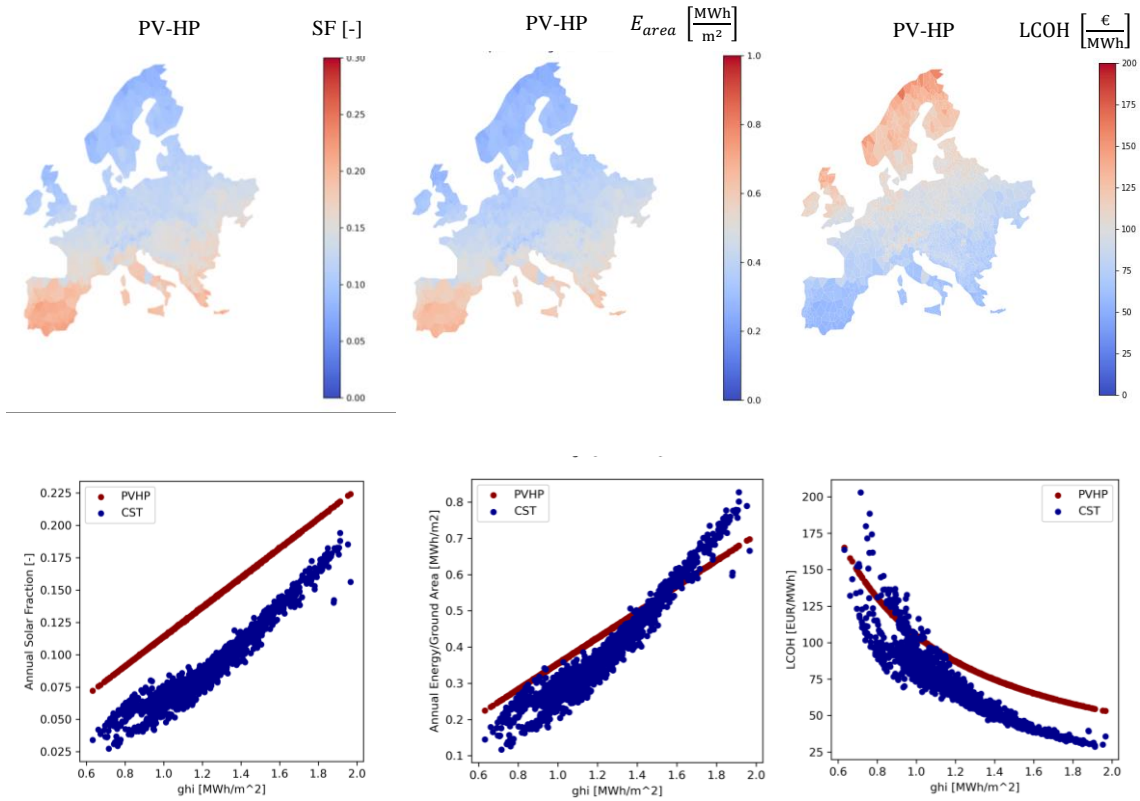


Fig.4: Comparative CST and PV-HP as heat sources for indirect steam generation in Europe.

For all the considered locations the PV-HP scheme provide higher solar fraction than CST, when assuming the same $SM = 1$. As expected solar fraction varies according with the GHI, increasing from 0.75 in the northern European locations up to 0.22 for southern locations for PV-HP, and from 0.03 to 0.20 for the CST case. As other energetic KPI it is worth to analyze the energy yield per unit of ground area. For high irradiance, GHI above 1.6 MWh/m^2 , corresponding to southern European locations, CST provides better results than PV-HP. In northern Europe the trend is reversed, and PV-HP provides higher values of E_{area} . Considering economics, the LCOH also is remarkably affected by solar resource, clearly decreasing with GHI. As general trend the cost of PV-HP is higher than the CST, which results the most convenient option, reaching values lower than 50 €/MWh in southern European locations.

4.2 Hybrid configuration

Although having slightly difference in the energetic or economic performance both CST and PV-HP are viable technologies for industrial steam generation. Both can be integrated in a hybrid solar steam generation layout, as in Fig. 3.

Annual simulations of hybrid scheme are carried out for several values of R_{hy} varying between 0 and 1, where $R_{hy} = 0$ corresponds to CST only and $R_{hy} = 1$ corresponding to PV-HP. As locations, 20 European sites are considered, representative of different climatic conditions.

Fig. 5 shows the results for a $SM_{hy} = 1$, so that no excess of energy is provided and TES is not included in the scheme. The annual solar fraction is shown against the global horizontal irradiation. Varying the hybridization ratio from 0 to 1 intermediate values between the CST and PV-HP reference cases are obtained either for the SF as for the LCOH.

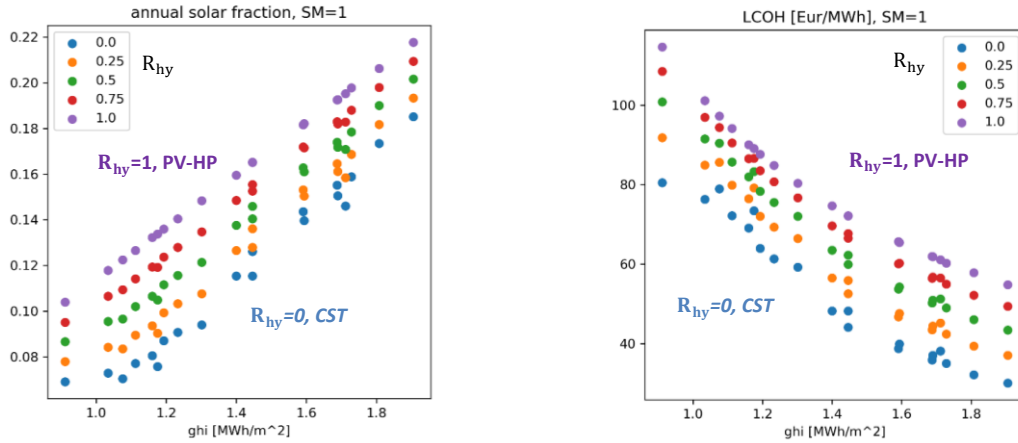


Fig.5: Hybrid scheme, with different hybridization ratios without TES

As previously mentioned, assuming the $SM_{hy} = 1$ limits the achievable solar fraction to relatively low values, having a top of 0.18-0.22 for high GHI locations in the south, and lower values going to northern sites. Increasing the solar multiple to $SM_{hy} > 1$ can lead to increased solar fraction but excess of energy appears in the central hours of the days especially in the summer season. The excess of energy, the energy provided by solar installation not absorbed instantaneously by the industrial process, can be stored if a proper TES is included into the layout as in Fig. 3. Depending on the TES size, the energy excess can be stored completely or partially, according to the installed storage capacity and the control strategy.

4.3 Hybrid configuration with TES

The results of TES sizing procedure are shown in terms of storage hours h_{TES} , Fig. 6, for $SM_{hy} = 3$ and for $SM_{hy} = 5$, for all the considered locations and hybridization ratio. For $SM = 3$ the h_{TES} varies from 0 to 6 according to location and hybridization ratio, as results of sizing procedure, while higher values up to $h_{TES} = 12$ are obtained for $SM_{hy} = 5$.

The resulting SF and LCOH are shown accordingly in Fig.6. Highest values of solar fraction still are associated with PV-HP, reaching $SF = 0.6$ for high GHI locations. Conversely, the best economic performance are related to CST, with small or null TES.

Increasing the oversizing of solar installation, for $SM_{hy} = 5$ a solar fraction of $SF = 0.8$ is reached at high GHI with PV-HP, decreasing going to lower R_{hy} and lower GHI. The economic trend is similar to previous case discussed, but higher LCOH is shown according to the added cost of TES. The best economic performance are obtained for $GHI = 1.9 \text{ MWh/m}^2$, with a $LCOH = 60 \div 85 \text{ €/MWh}$ with $SF = 0.67 \div 0.8$, with more than 10 hr of storage.

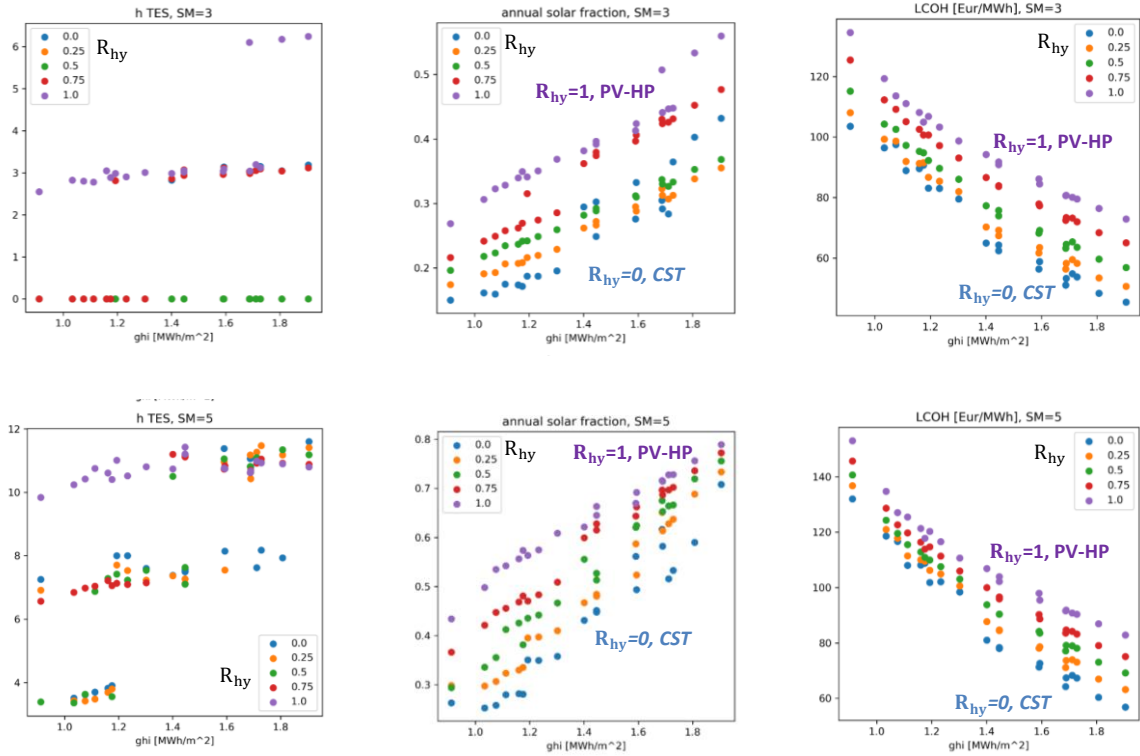


Fig. 6: Hybrid configuration with TES

5. Conclusions

An energetic and economic analysis is carried out on the industrial solar steam generation using linear Fresnel solar collectors (CST) and high temperature heat pump powered by dedicated photovoltaic (PV-HP). Steam production at 8 bar is analysed through numerical annual simulation for several locations in Europe. A comparative analysis between CST and PV-HP indicates that higher annual solar fraction can be obtained using PV-HP respect to CST, assuming a unitary solar multiple. Considering the actual cost of the technologies, a lower LCOH is shown by CST option.

Moreover, the possibility of implementing hybrid layout including either CST and PV-HP as heat source varying the main design parameters is analysed across European locations. The limitation of low annual solar fraction can be overcome by oversizing the solar installations and including a sensible thermal energy storage TES. According to the design criterion implemented in the study, simulations for different solar multiple are carried out as basis for an economic and energetic assessment. The hybrid scheme with TES allows high solar fraction with an increased cost associated with the cost of thermal storage.

6. Acknowledgments

This research was supported by the Industrial Ph.D. program of Comunidad de Madrid, Spain (BOCM Reference IND2017/ AMB7769), “Ayudas Juan de la Cierva Formación de Ministerio de Ciencia e Innovación” funded by MCIN/AEI/10.13039/501100011033 and European Union “NextGenerationEU”/PRTR, and Open-Seed Funds 2023 by Pontificia Universidad Catolica de Chile, Title: “Development of a simulation tool for yield assessment of solar heat for industrial processes coupled to thermal energy storage”.

7. References

- Annex 58 Task 1. (n.d.). Retrieved July 15, 2024, from <https://heatpumpingtechnologies.org/annex58/task1/>
- Arpagaus, C., Bless, F., Uhlmann, M., Schiffmann, J., & Bertsch, S. S. (2018). High temperature heat pumps: Market overview, state of the art, research status, refrigerants, and application potentials. In *Energy* (Vol. 152, pp. 985–1010). Elsevier Ltd. <https://doi.org/10.1016/j.energy.2018.03.166>
- Burkholder, F., & Kutscher, C. F. (2009). Heat loss testing of Schott's 2008 PTR70 parabolic trough receiver. *NREL Technical Report, May*, 58. <http://www.nrel.gov/docs/fy09osti/45633.pdf>
- Duffie, J. A., Beckman, W. A., & McGowan, J. (1985). Solar Engineering of Thermal Processes. In *American Journal of Physics* (Vol. 53, Issue 4). <https://doi.org/10.1119/1.14178>
- Høeg, A., Løver, K., Asphjell, T.-A., & Lümmen, N. (2023). *Performance of a new ultra-high temperature industrial heat pump*. <https://www.researchgate.net/publication/371192209>
- Enerin. Retrieved July 15, 2024, from <https://www.enerin.no/>
- International Renewable Energy Agency (IRENA). (n.d.). www.irena.org
- Maxwell, C. *Cost indices. 2024*. URL: <https://toweringskills.com/financial-analysis/cost-indices/>; accessed: 2024.
- Mostafavi Tehrani, S. S., Taylor, R. A., Nithyanandam, K., & Shafiei Ghazani, A. (2017). Annual comparative performance and cost analysis of high temperature, sensible thermal energy storage systems integrated with a concentrated solar power plant. *Solar Energy*, 153, 153–172. <https://doi.org/10.1016/j.solener.2017.05.044>
- Solatom. *SOLAR STEAM FOR INDUSTRIAL PROCESSES*. <http://www.solatom.com/>